

Functionalized graphene oxide based on *p*-phenylenediamine as spacers and nitrogen dopants for high performance supercapacitors

Yanhong Lu · Yi Huang · Fan Zhang ·
Long Zhang · Xi Yang · Tengfei Zhang ·
Kai Leng · Mingjie Zhang · Yongsheng Chen

Received: 25 October 2013 / Accepted: 21 January 2014 / Published online: 2 April 2014
© Science China Press and Springer-Verlag Berlin Heidelberg 2014

Abstract *p*-Phenylenediamine (PPD) functionalized graphene oxide (GO) materials (PPDG) were prepared through a one-step solvothermal process and their application as supercapacitors (SCs) were studied. The PPD is not only as the spacers to prevent aggregating and restacking of the graphene sheets in the preparing process but also as nitrogen sources to obtain the nitrogen-doped graphene. The structures of PPDG were characterized by Fourier transformed infrared spectroscopy (FT-IR), X-ray diffraction spectroscopy (XRD), Raman spectroscopy and X-ray photoelectron spectroscopy (XPS) and the results show that the nitrogen-doped graphene was achieved with nitrogen content as high as 10.85 at.%. The field emission scanning electron microscopy (FE-SEM) and high resolution transmission electron microscopy (HR-TEM) have confirmed that the morphologies of PPDG were loose

layered with less aggregation, indicating that PPD molecules, as spacers, effectively prevent the graphene sheets from restacking during the solvothermal reaction. The special loose textures make PPDG materials exhibit excellent electrochemical performance for symmetric SCs with superior specific capacitance (313 F/g at 0.1 A/g), rate capability and cycling stability. The present synthesis method is convenient and may have potential applications as ultrahigh performance SCs.

Keywords Graphene · *p*-phenylenediamine · Supercapacitor · Functionalized · Nitrogen-doped

1 Introduction

Supercapacitors (SCs), also called electrochemical capacitors and ultracapacitors, are increasingly important owing to their fascinating physical and chemical properties of high power density, ultra-long cycle life, and rapid charge/discharge rates [1, 2]. Based on the charge storage mechanism, SCs can be divided into pseudo-capacitors and electrical double layer capacitors (EDLCs) [3]. The performance of the SCs highly depends on the properties of electrode materials [4]. Graphene, a flexible 2-dimensional (2D) single-layer sheet of sp^2 -hybridized carbon material, has recently attracted great interests for SCs applications because of its excellent and unique properties, such as good chemical stability, high electrical conductivity and large surface area [5–8]. Unfortunately, the individual graphene sheets tend to form irreversible aggregation or restacking during the solvothermal reduction process because of the π - π stacking, leading to a dramatic decrease in the surface area and lower electrochemical performance [9]. Therefore, how to efficiently prevent the irreversible aggregation and minimize the restacking effect is of great importance

SPECIAL TOPIC: Nano Materials

Y. Lu (✉)
School of Chemistry & Material Science, Langfang Teachers College, Langfang 065000, China
e-mail: luyanhong_2003@126.com

Y. Lu · Y. Huang (✉) · F. Zhang · L. Zhang · X. Yang · T. Zhang · K. Leng · M. Zhang · Y. Chen (✉)
Collaborative Innovation Center of Chemical Science and Engineering (Tianjin), Key Laboratory of Functional Polymer Materials and Center for Nanoscale Science and Technology, Institute of Polymer Chemistry, College of Chemistry, Nankai University, Tianjin 300071, China
e-mail: yihuang@nankai.edu.cn

Y. Chen
e-mail: yschen99@nankai.edu.cn

Y. Lu · M. Zhang
Department of Chemistry, School of Sciences, Tianjin University, Tianjin 300072, China

to improve the performance of graphene-based SCs and expand the applications of graphene [10]. Many methods [11–13] and feasible active species have been used as spacers. Carbon nanotubes (CNT) [14, 15] are extremely attractive due to their outstanding properties. But CNT themselves cannot offer the capacitance performance and the specific capacitance (C_{sp}) of their composite materials based SCs are low (190 and 120 F/g [10, 11]). Although the high C_{sp} value of 3-dimensional CNT/graphene based SCs was obtained by Fan et al. (385 F/g at 10 mV/s) [16] and Yang et al. (326 F/g at 20 mV/s) [17], several problems still need to be addressed in terms of complicated synthesis procedures, waste of time and requirement of high temperatures. Conducting polymers [18, 19], and metal oxides [20–22] could be served as fillers and simultaneously enhanced the C_{sp} value. But the capacitance of the composites based SCs would easily decay, due to the volume change and ion dissolution during charge/discharge processes. Chen et al. [23] used organic amine as spacers and nitrogen sources, which could form electrochemical active groups and provide the pseudo-capacitance. However, the C_{sp} is only 190.1 F/g. Ai et al. [24] reported an efficient method for the synthesis of covalently functionalized graphene materials, with less aggregation and abundant redox active azole functional groups and higher C_{sp} (730 F/g at 0.1 A/g), but the C_{sp} value has a sharp decrease with the current density enhanced, which is 296 F/g at 0.8 A/g and only 40 % is retained, indicating the rate capability couldn't satisfied to the applications.

In this study, *p*-phenylenediamine (PPD) functionalized graphene oxide (GO) composite materials (PPDG) were obtained through one-pot solvothermal process. On one hand, PPD molecules could insert the space in between the graphene sheets through the reactions of $-NH_2$ on the para-position of benzene ring and the different graphene sheets, respectively (Fig. 1). Thus PPD molecules are as spacers to control the aggregation and restacking of graphene sheets and formed loose layered structures, which is favorable to the diffusion of electrolyte ion, leading to a great improvement of the electrochemical performance for SCs. On the other hand, PPD molecules can serve as nitrogen dopants to realize nitrogen doping, which further enhanced the performance of the electrode materials. The PPDG based SCs (PPDG-SCs) exhibit ultrahigh C_{sp} value of 313 F/g at 0.1 A/g in 6 mol/L KOH aqueous solution, superior rate capability and cycling stability. The materials may have potential applications as ultrahigh performance SCs.

2 Experimental

2.1 Materials synthesis

GO and PPDG was synthesized according to our previous reported method [25, 26]. Typically, PPD ethanol solution

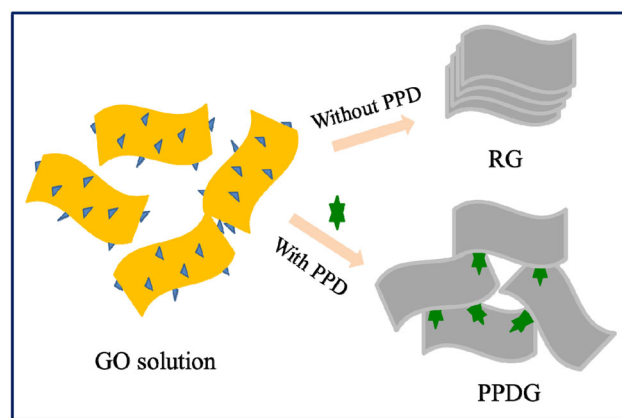


Fig. 1 (Color online) Schematic illustration for the synthesis of RG and PPDG materials

(10 mg/mL) was added to 40 mL GO aqueous solution (4 mg/mL). The mixture solution was ultrasonicated for 0.5 h and then transferred to a 100 mL autoclave. Solvothermal reaction was at 180 °C for 12 h. The autoclave was then naturally cooled to room temperature. The product was washed several times with ethanol and acetone by filtrate. Finally, the sample was dried in a vacuum oven at 120 °C for 12 h. For comparison, reduced GO (RG) was also prepared under the same experimental parameters but without adding PPD.

2.2 Characterization

The morphology of the products was investigated by a field emission scanning electron microscopy (FE-SEM, LEO 1530 VP) and high resolution transmission electron microscopy (TEM, JEOL TEM-2100). Raman scattering was carried out on a Renishaw inVia Raman spectrometer using laser excitation at 633 nm. Fourier transform infrared (FT-IR) spectra were recorded on a Bruker Tensor 27 spectrometer (Germany). X-ray photoelectron spectroscopy (XPS) analysis was performed using AXIS HIS 165 spectrometer (Kratos Analytical) with a monochromatized Al K α X-ray source (1486.71 eV photons).

2.3 Fabrication of supercapacitors and electrochemical measurements

The SCs test cells were fabricated according to our reported method [27, 28]. The electrode materials were prepared by mixing PPDG or RG, carbon black and polytetrafluoroethylene at the weight ratio of 85:5:10. The mixture was homogenized and then was rolled into 80–120 μ m thickness sheets and punched into 13 mm diameter, and was dried at 120 °C for 6 h under vacuum. The Ni foam was as the current collector, the cellulose film was as the separator and 6 mol/L KOH aqueous solution

was used as electrolyte. The CV curves were studied with a LK98B II microcomputer-based electro-chemical analyzer (LANLIKE). The galvanostatic charge/discharge was performed with a supercapacitor tester (Arbin MSTAT, USA). Electrical impedance spectroscopy (EIS) studies were obtained by a frequency response analysis of the frequency range from 10 mHz to 100 kHz using Autolab (Metrohm). The C_{sp} value was calculated according to our previous reported method [29].

3 Results and discussion

The morphology of RG and PPDG was characterized by SEM and TEM. As shown in Fig. 2a, the SEM image of RG shows a tight aggregated structure. However PPDG has an extremely loose layered and silk-like structure (Fig. 2b), indicating the effectiveness of PPD for the prevention of restacking of graphene sheets, supporting the below XRD results. This structure of PPDG should be available to the diffusion of electrolyte ion not only in the outer region of the graphene but also the inner region. So both sides of a broad range of graphene sheets could be exposed to the

electrolyte and thus contribute to the capacitance. The nitrogen content was studied by energy dispersive spectroscopy (EDS) and it reaches as high as 10.85 at.%. The nitrogen distribution in PPDG was confirmed by elemental mapping by SEM (Fig. 2d) and the results show that the whole basal plane of graphene sheets contain a large amount of nitrogen with a uniform distribution density, indicating a homogenous reaction between GO and PPD. The TEM characterization result (Fig. 3a) demonstrates the PPDG has ultra-thin sheet-like, crumpled and flexible structure.

To investigate the chemical structure of PPDG, Raman, FT-IR and XPS analyses of RG and PPDG were performed. The Raman spectra of RG and PPDG (Fig. 3b) display two peaks at 1324 and 1581 cm⁻¹, corresponding to the D and G bands respectively [30]. The I_D/I_G ratio is associated with disordered structures. As shown in Fig. 3b, after GO was functionalized with PPD, the I_D/I_G ratio increased from 0.95 for RG to 1.08 for PPDG, which can be ascribed to the increased defect sites created on graphene upon nitrogen doping [31, 32]. The FT-IR spectra of RG and PPDG were shown in Fig. 3c. For RG, the adsorption band appear at 1724, 1567 and 1201 cm⁻¹, corresponding to the

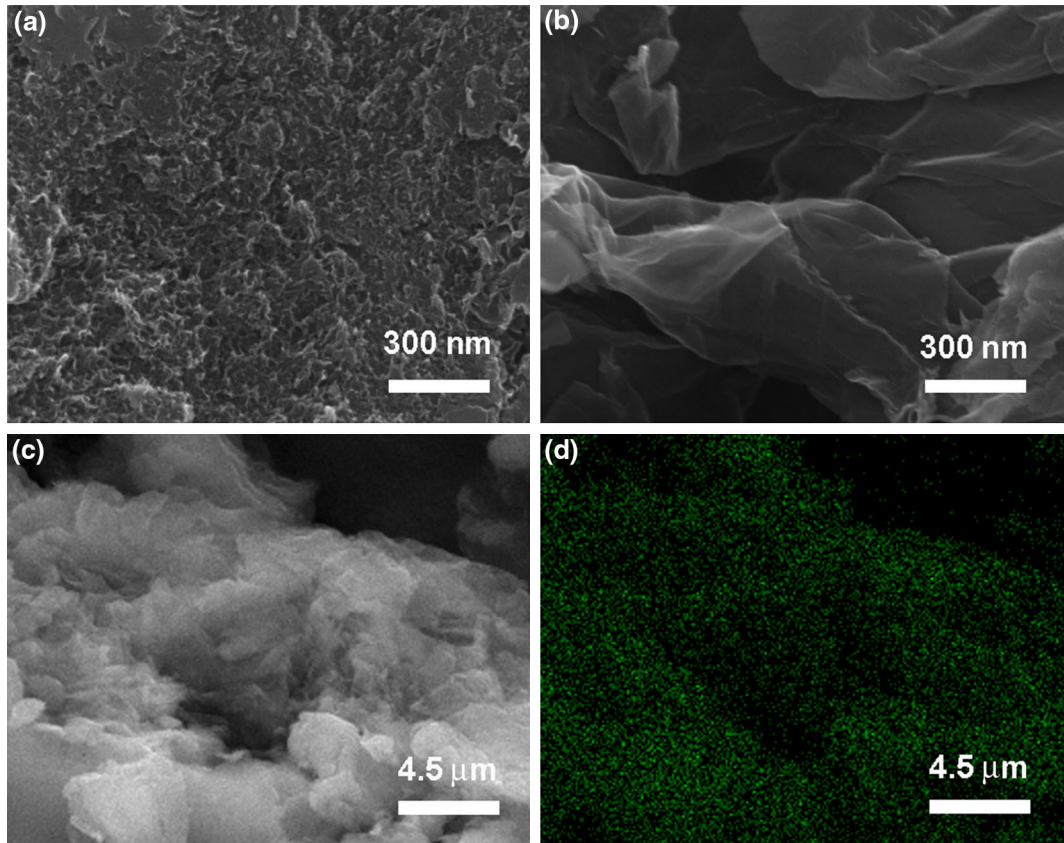


Fig. 2 (Color online) SEM images of (a) RG; (b, c) PPDG and (d) nitrogen mapping image of PPDG for (c)

carbonyl stretching mode, C=C stretching vibration of benzene bring and the breathing vibration mode of the epoxy groups, respectively [33]. However, in the spectrum of PPDG, the peaks at 1724 cm^{-1} disappear, which may be explained that the oxygen containing functional groups in GO would react with the $-\text{NH}_2$ in PPD to generate other covalent bonds. Moreover, a new peak at 1388 cm^{-1} is observed, which is attributed to the stretching mode of C=N and C=N bonds [34]. Furthermore, the peaks at around

1100 cm^{-1} results from the stretching of C–N bonds and the residual C–O groups [35]. XPS was then underutilized to determine the configurations of nitrogen in PPDG, shown in Fig. 4. The full range XPS of RG (Fig. 4a) reveals the presence of C1s (284 eV) and O1s (532 eV), while in the spectrum of PPDG, the peak of N1s (399 eV) was present, indicating the nitrogen had introduced to the graphene sheets. The high-resolution C1s spectrum of RG shows three different peaks (Fig. 4b). The peaks at

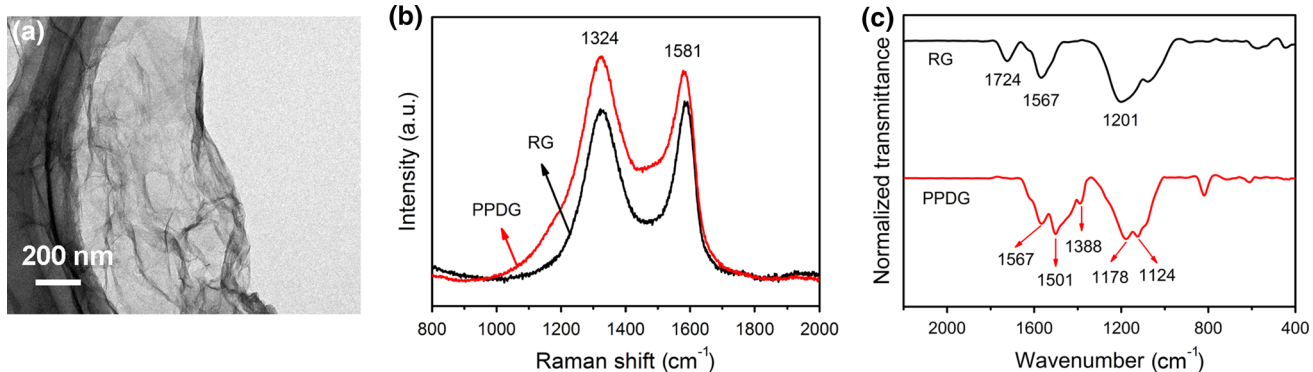


Fig. 3 (Color online) (a) TEM image of PPDG; (b) Raman spectra of RG and PPDG and (c) FT-IR spectra of RG and PPDG

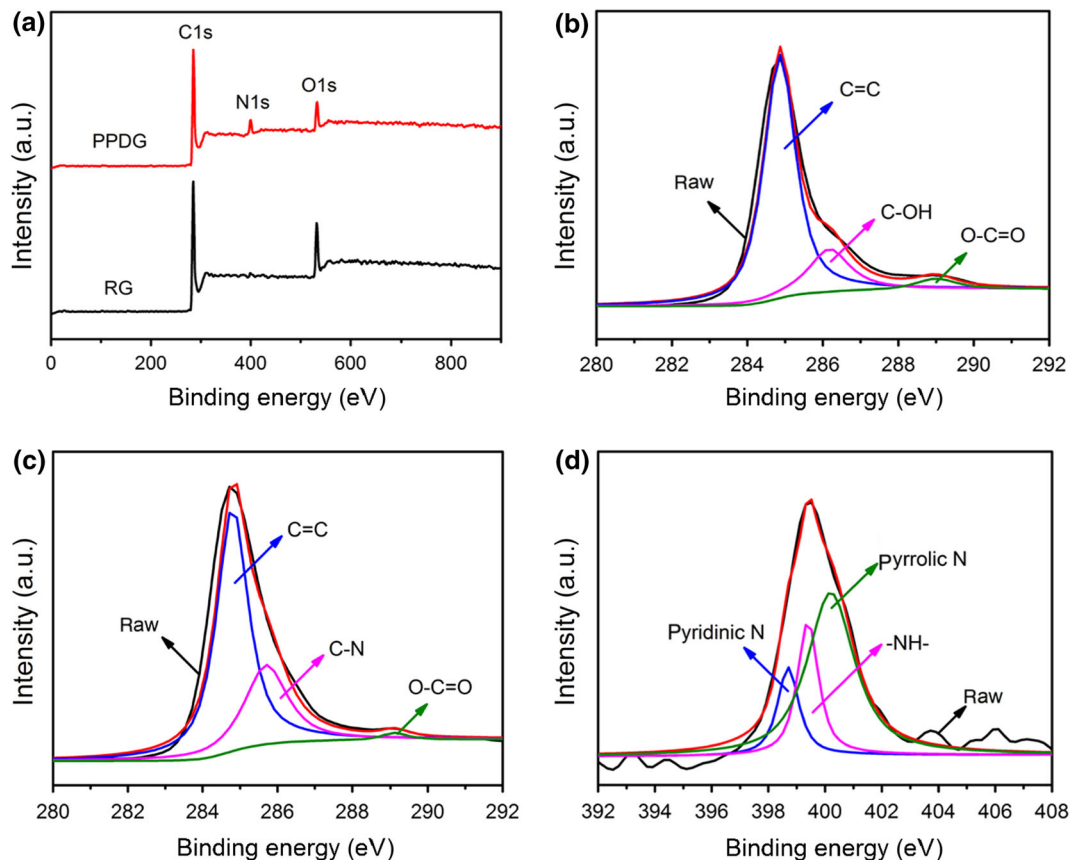


Fig. 4 (Color online) XPS spectra of (a) Survey spectra of RG and PPDG; (b) High resolution C1s spectra of RG and (c) PPDG; (d) N1s spectra of PPDG

284.8, 286.2 and 289.0 eV correspond to the sp^2 carbon ($\text{C}=\text{C}$), $\text{C}-\text{OH}$ and $\text{O}-\text{C}=\text{O}$, respectively [19]. While in the high-resolution C1s spectrum of PPDG (Fig. 4c), the appearance of a new peak at 285.7 eV ($\text{C}=\text{N}$) further confirms the presence of nitrogen in the graphene sheets [36]. The bonding configurations of nitrogen atoms in PPDG were further investigated by high-resolution N 1s XPS spectra (Fig. 4d), showing three different types of nitrogen atoms with binding energies of 398.7, 399.4 and 400.2 eV, which is attributed to pyridinic nitrogen, amine moieties or other sp^3 -C and nitrogen bonds and pyrrolic nitrogen, respectively [37].

In order to investigate the electrochemical performance of PPDG materials, a two-electrode cell with a symmetrical configuration was performed. The electrochemical properties of PPDG-SCs with the contrastive one's (RG-SCs) were analyzed by CV and galvanostatic charge/discharge techniques. Figure 5a shows the CV curves of RG-SCs at scan rate of 10 mV/s and PPDG-SCs at the scan rates of 10, 20 and 50 mV/s in 6 mol/L KOH aqueous electrolyte. Obviously, a

much higher capacitive response of PPDG-SCs is observed, suggesting that the electrochemical activity of graphene materials is increased after functionalization by PPD. Moreover, in contrast with the pure capacitive current background in CV curve of RG-SCs, the Faradic redox peaks of PPDG-SCs appear, whatever at low or high scan rates, which may correspond to the redox reactions of the electrochemically active functional groups, including pyridinic nitrogen and pyrrolic nitrogen groups on the functional graphene sheets. The galvanostatic charge/discharge curves of PPDG-SCs at different current densities were shown in Fig. 5b. The C_{sp} value for PPDG-SCs is 313 F/g at a constant current of 0.1 A/g, which is much higher than that of RG-SCs (210 F/g). Furthermore, PPDG-SCs also display a superior rate capability (Fig. 5c). The electrochemical impedance spectroscopy (EIS) was also performed. As shown in Fig. 6a, the Nyquist plots of both RG-SCs and PPDG-SCs have the lower equivalent series resistance (ESR, intercept on the x axis) at high frequency, which represents that the intrinsic internal resistance of the electrode materials and electrolyte of RG-

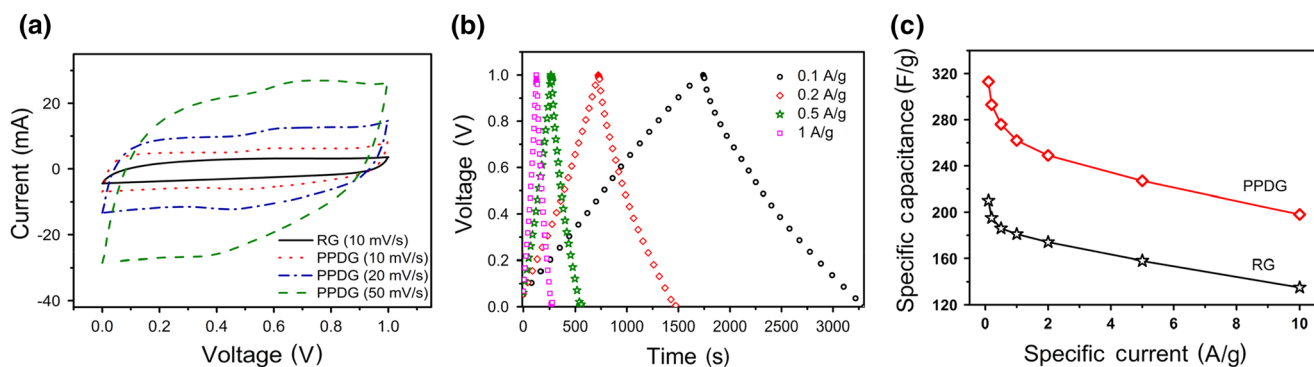


Fig. 5 (Color online) Electrochemical performance of the SCs: (a) CV curves of RG-SCs measured at the scan rate of 10 mV/s and PPDG-SCs measured at the scan rates of 10, 20 and 50 mV/s in the potential range of 0–1.0 V; (b) Galvanostatic charge/discharge curves for PPDG-SCs tested at current densities from 0.1 to 1 A/g; (c) Rate performances of PPDG-SCs and RG-SCs

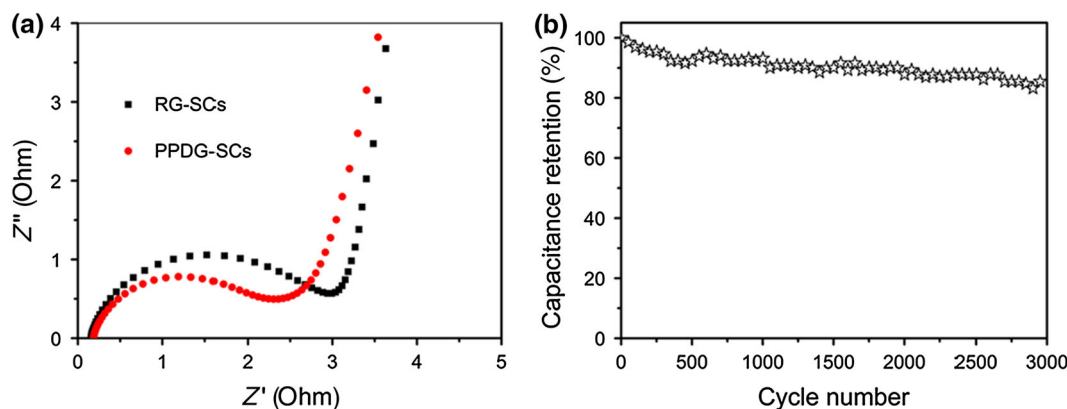


Fig. 6 (Color online) (a) Nyquist impedance plots of RG-SCs and PPDG-SCs; (b) cycling stabilities for PPDG-SCs charge-discharged after 3000 cycles, measured at a current density of 1 A/g within the potential range from 0 to 1.0 V

SCs and PPDG-SCs are small [25]. However, compared with the RG-SCs, the PPDG-SCs exhibit a much smaller the radius of semicircle plotted at the high to mid frequency region, indicating the lower charge-transfer resistance and better conductivity of PPDG materials [38], which may contributed by the loose layer graphene structures. Cycling performance of the PPDG-SCs was evaluated using galvanostatic charge/discharge technique at a current density of 1.0 A/g (Fig. 6b). As can be seen, PPDG-SCs exhibit only 15 % deterioration of the initial C_{sp} after 3000 cycles, indicating the good cycling stabilities. The excellent electrochemical performance of PPDG-SCs could be ascribed to the morphology and structure of PPDG. On one hand, the PPD molecules, using as spacers, could prevent GO restacking in the solvothermal process and form the loose layered structure, which are favorable for the electrolyte penetration and accelerate the kinetic process of the ion diffusion and enhance the performance. One the other hand, nitrogen-doped graphene, with abundant pyridinic and pyrrolic structures, which could provide the pseudo-capacitance, could be obtained through the introduction of PPD. So the unique structures endow rapid transport of the electrolyte ions and simultaneously utilize the pseudo- and double layer capacitance.

4 Conclusions

We have prepared PPD functionalized graphene materials with loose layered structures and nitrogen doping through one-pot solvothermal process. The pyridinic nitrogen and pyrrolic nitrogen formed in the doping process. Because of their less aggregated and loose layered structures, high content of nitrogen atoms and appropriate nitrogen species, the prepared materials display a high C_{sp} up to 313 F/g in addition to maintaining excellent rate capability and cycling stability. Therefore, the PPDG materials could be applied for high-performance SCs.

Acknowledgements This work was supported by the Ministry of Science and Technology (2012CB933401, 2014CB643502), the National Natural Science Foundation of China (51273093, 21374050, 51373078), Natural Science Foundation of Tianjin (10ZCGHHZ00600), the Synergetic Innovation Center of Chemical Science and Engineering (Tianjin), Science and Technology Research Project of Higher Education of Hebei Province (z2012064), and Science Research Project of Langfang Teachers College (LSZQ200908).

References

- Zhu YW, Murali S, Stoller MD et al (2011) Carbon-based supercapacitors produced by activation of graphene. *Science* 332:1537–1541
- Liu C, Li F, Ma LP et al (2012) Advanced materials for energy storage. *Adv Mater* 22:E28–E62
- Huang Y, Liang JJ, Chen YS (2012) An overview of the applications of graphene-based materials in supercapacitors. *Small* 8:1805–1834
- Simon P, Gogotsi Y (2008) Materials for electrochemical capacitors. *Nat Mater* 7:845–854
- Stoller MD, Park S, Zhu YW et al (2008) Graphene-based ultracapacitors. *Nano Lett* 8:3498–3502
- Zhang L, Yang X, Zhang F et al (2013) Controlling the effective surface area and pore size distribution of sp^2 carbon materials and their impact on the capacitance performance of these materials. *J Am Chem Soc* 135:5921–5929
- Wang Y, Shi ZQ, Huang Y et al (2009) Supercapacitor devices based on graphene materials. *J Phys Chem C* 113:13103–13107
- Leng K, Zhang F, Zhang L et al (2013) Graphene-based Li-ion hybrid supercapacitors with ultrahigh performance. *Nano Res* 6:581–592
- Yan J, Xiao Y, Ning GQ et al (2013) Facile and rapid synthesis of highly crumpled graphene sheets as high-performance electrodes for supercapacitors. *RSC Adv* 3:2566–2571
- Song FQ, Li ZY, Wang ZW et al (2010) Free-standing graphene by scanning transmission electron microscopy. *Ultramicroscopy* 110:1460–1464
- Liao KM, Ding WF, Zhao B et al (2011) High-power splitting of expanded graphite to produce few-layer graphene sheets. *Carbon* 49:2862–2868
- Wei DC, Liu YQ, Zhang HL et al (2009) Scalable synthesis of few-layer graphene ribbons with controlled morphologies by a template method and their applications in nanoelectromechanical switches. *J Am Chem Soc* 131:11147–11154
- Nuvoli D, Valentini L, Alzari V (2011) High concentration few-layer graphene sheets obtained by liquid phase exfoliation of graphite in ionic liquid. *J Mater Chem* 21:3428–3431
- Wang Y, Wu YP, Huang Y et al (2011) Preventing graphene sheets from restacking for high-capacitance performance. *J Phys Chem C* 115:23192–23197
- Yu DS, Dai LM (2010) Self-assembled graphene/carbon nanotube hybrid films for supercapacitors. *J Phys Chem Lett* 1:467–470
- Fan ZJ, Yan J, Zhi LJ et al (2010) A three-dimensional carbon nanotube/graphene sandwich and its application as electrode in supercapacitors. *Adv Mater* 22:3723–3728
- Yang SY, Chang KH, Tien HW et al (2011) Design and tailoring of a hierarchical graphene-carbon nanotube architecture for supercapacitors. *J Mater Chem* 21:2374–2380
- Wang DW, Li F, Zhao JP et al (2009) Fabrication of graphene/polyaniline composite paper via in situ anodic electropolymerization for high-performance flexible electrode. *ACS Nano* 3:1745–1752
- Yan J, Wei T, Shao B et al (2010) Preparation of a graphene nanosheet/polyaniline composite with high specific capacitance. *Carbon* 48:487–493
- Zhou GM, Wang DW, Li F et al (2010) Graphene-wrapped Fe_3O_4 anode material with improved reversible capacity and cyclic stability for lithium ion batteries. *Chem Mater* 22:5306–5313
- Yan J, Sun W, Wei T et al (2012) Fabrication and electrochemical performances of hierarchical porous $Ni(OH)_2$ nanoflakes anchored on graphene sheets. *J Mater Chem* 22:11494–11502
- Wei Lv, Sun F, Tang DM et al (2011) A sandwich structure of graphene and nickel oxide with excellent supercapacitive performance. *J Mater Chem* 21:9014–9019
- Chen P, Yang JJ, Li SS et al (2013) Hydrothermal synthesis of macroscopic nitrogen-doped graphene hydrogels for ultrafast supercapacitor. *Nano Energy* 2:249–256
- Ai W, Zhou WW, Du ZZ et al (2012) Benzoxazole and benzimidazole heterocycle-grafted graphene for high-performance supercapacitor electrodes. *J Mater Chem* 22:23439–23446

25. Yang X, Zhang F, Zhang L et al (2013) A high-performance graphene oxide-doped ion gel as gel polymer electrolyte for all-solid-state supercapacitor application. *Adv Funct Mater* 23: 3353–3360
26. Lu YH, Zhang F, Zhang TF et al (2013) Synthesis and supercapacitor performance studies of N-dope graphene materials using o-phenylenediamine as the double-N precursor. *Carbon* 63:508–516
27. Zhang F, Zhang TF, Yang X et al (2013) A high-performance supercapacitor-battery hybrid energy storage device based on graphene-enhanced electrode materials with ultrahigh energy density. *Energy Environ Sci* 6:1623–1632
28. Zhang L, Zhang F, Yang X et al (2013) Porous 3D graphene-based bulk materials with exceptional high surface area and excellent conductivity for supercapacitors. *Sci Rep* 3:1408–1416
29. Zhang L, Zhang F, Yang X et al (2013) High-performance supercapacitor electrode materials prepared from various pollens. *Small* 9:1342–1347
30. Lv W, Tang DM, He YB et al (2009) Low-temperature exfoliated graphenes vacuum-promoted exfoliation and electrochemical energy storage. *ACS Nano* 3:3730–3736
31. Guo HL, Su P, Kang XF et al (2013) Synthesis and characterization of nitrogen-doped graphene hydrogels by hydrothermal route with urea as reducing-doping agents. *J Mater Chem A* 1:2248–2255
32. Gao H, Song L, Guo WH et al (2012) A simple method to synthesize continuous large area nitrogen-doped graphene. *Carbon* 50:4476–4482
33. Hu NT, Wang YY, Chai J et al (2012) Gas sensor based on p-phenylenediamine reduced graphene oxide. *Sensor Actuat B* 163:107–114
34. Xue YH, Liu J, Chen H et al (2012) Nitrogen-doped graphene foams as metal-free counter electrodes in high-performance dye-sensitized solar cells. *Angew Chem* 124:12290–12293
35. Lin ZY, Waller G, Liu Y et al (2012) Facile synthesis of nitrogen-doped graphene via pyrolysis of graphene oxide and urea, and its electrocatalytic activity toward the oxygen-reduction reaction. *Adv Energy Mater* 2:884–888
36. Unni SM, Devulapally S, Karjulea N et al (2012) Graphene enriched with pyrrolic coordination of the doped nitrogen as an efficient metal-free electrocatalyst for oxygen reduction. *J Mater Chem* 22:23506–23513
37. Lee JW, Ko JM, Kim JD (2012) Hydrothermal preparation of nitrogen-doped graphene sheets via hexamethylenetetramine for application as supercapacitor electrodes. *Electrochim Acta* 85:459–466
38. Sun L, Wang L, Tian CG et al (2012) Nitrogen-doped graphene with high nitrogen level via a one-step hydrothermal reaction of graphene oxide with urea for superior capacitive energy storage. *RSC Adv* 2:450–4498